Bilateral Gaussian Wake Model Formulation for Wind Farms: A Forecasting Based Approach

Harsh S. Dhiman[a], Dipankar Deb[a], Aoife M. Foley[b]

[a]*Department of Electrical Engineering, Institute of Infrastructure Technology Research and Management, Ahmedabad, India 380026.*
[b]*School of Mechanical and Aerospace Engineering, Queens University, Belfast, Northern Ireland, United Kingdom*

Abstract

Wind energy installations require precise study of land area available and prevailing nearby atmospheric conditions. The power captured from wind resource is dependent on wind speed at the site. Optimal placement of wind turbines in a wind farm to yield maximum power capture in presence of wind wakes is a major challenge. In this paper, a bilateral Gaussian wake model based approach is formulated using Gaussian variations of well established Jensen's and Frandesen's model. This proposed model is such that the incident wind speed on a downwind turbine due to wake effect from upwind turbines is minimized. The proposed model is compared with benchmark analytical models for single and multiple wake scenarios. Furthermore, short-term wind speed forecasting in presence of wakes is carried out for two wind farm layouts considering benchmark wake models and our proposed model. The significant upwind turbines are identified for two wind farm layouts using Grey relational analysis, and the forecasting accuracy is evaluated for the proposed model and benchmark wake models.

Keywords: Grey relational analysis, Jensen's model, Short-term wind forecasting, Support vector regression, Wind farm layout, Wind wakes

*Harsh S. Dhiman
Email addresses: harsh.dhiman.17pe@iitram.ac.in (Harsh S. Dhiman), dipankardeb@iitram.ac.in (Dipankar Deb), a.foley@qub.ac.uk (Aoife M. Foley)

Abbreviations

ABL	Atmospheric Boundary Layer
ARMA	Autoregressive Moving Average
ARIMA	Autoregressive Moving Integrated Moving Average
ANN	Artificial Neural Network
CFD	Computational Fluid Dynamics
GRA	Grey Relational Analysis
LES	Large-eddy Simulation
RMSE	Root Mean Squared Error
SVR	Support vector regression
WFLOP	Wind Farm Layout Optimization

1. Introduction

Growing energy demands are rapidly facilitating the wind turbine installations globally in the form of large wind parks. Wind turbines are installed in large land mass to convert the energy available from moving air to electrical energy. Due to constrained land area and cost of the equipment one has to design a proper wind farm layout for the required energy generation [1]. Wind power capture by wind turbine is affected by many factors like wind speed, wind direction and optimal turbine spacing [2].

In a wind farm terrain, wind turbines must be placed at an optimal operating distance from each other to avoid potential derating caused by wind wakes. Wind wake is an aerodynamic phenomenon leading to (a) reduction in wind speed magnitude at the downwind turbine, and (b) increased air turbulence causing mechanical loading on the turbine structure [3]. Wind wakes can be classified as near-end wakes and far-end wakes, former extends up to a distance of one to three rotor diameters where the flow is dependent on the turbine

geometry [4]. Early wake models were developed in 1980's with N.O. Jensen proposing single wake model describing wind speed deficit caused by a single upwind turbine on downwind turbine. Various analytical models like Ainslie's model [5], Larsen's model [6] and Frandsen's model [7] have been used. Most commonly used model is the Jensen's model that assumes linear wake expansion after the hub. Ainslie's wake model considers a numerical wake model with symmetric Reynolds equation to compute wake development and found that wake deficit decays monotonically with increasing downstream distance (experimentally 4D) [8]. However the computation time of Ainslie's model was found to be large [9]. A new 2-D Jensen wake model is proposed by Tian et al. that incorporates the variable wake decay rate rather than a constant one. Numerical simulations are performed for computing the wake deficit and are compared with field measurements. Results reveal that the proposed 2-D Jensen wake model generally underestimates for near-wake regions [10]. Ishihara et al. have presented an analytical model that encapsulates the effect of thrust coefficient and air turbulence on the wake deficit [11]. The numerical simulations are compared with a test carried out in wind tunnel and results of the proposed analytical model are in good agreement with experimental analysis. In terms of Large-eddy simulation (LES), the wake flow is studied in neutral atmospheric boundary layer, where the aerodynamic effects acting on the rotor body and blade element are modeled separately in order to assess the power losses inside wind farms [12, 13, 14].

Computational fluid dynamics (CFD) based wake models have been used actively over past years to model the far-end wake characteristics typically for a HAWT configuration. Rethore et al. have discussed a canopy model for modelling the atmospheric turbulence where the kinetic energy lost in aerodynamics is transferred into turbulence [15]. The performance of analytical model is found superior to that of standard $k-\omega$ model. Further, Stergiannis et al. have presented CFD simulations of two turbines placed at a longitudinal distance of 2.77D, 5.17D and 9D, where D=0.89m is the rotor diameter, are carried out [16]. Three test conditions are generated with low turbulence intensity uniform

flow, high turbulence intensity uniform flow and high turbulence shear inflow. A uniform velocity of 11.5 m/s is maintained at test inlet. Results reveal that Actuator disk model under- predicts the wake velocity for $k-\omega$ and $k-\varepsilon$ turbulence models.

Wind wakes causing power loss for an individual wind turbine leads to detailed study of wind wakes and hence over the years many analytical and field models have been developed to study the same [17]. Experimental results have shown that due to wake interference the downwind turbine experiences up to 40% of power loss and 80% of increased dynamic loading on the turbine structure [18] where in wind turbine with rotor diameter 0.9 m is placed 4 rotor diameters from the wind inlet section, and wake velocity distribution is measured at a downstream distance of 0.6D and 3D. Jensen's wake model is validated and tested for accommodating the power losses in wind and the losses are found to be in acceptable range [19, 20, 21]. Wake study also plays an important role in Wind Farm Layout Optimization Problem (WFLOP) where optimal placement of the wind turbines leads to to minimum wake effect and maximum power capture [22].

Wind being stochastic in nature, its accurate forecasting is a major challenge in power industry. Wind speed forecasting has become an essential component to ensure power system security and reliability as increased wind power penetration will lead to an unreliable operation [23]. It also serves the purpose of market clearing operations and efficient load dispatch planning. Wind forecasting is broadly categorized on the basis of prediction horizon, that is, very short-term (few seconds to 30 minutes), short-term (30 minutes to 6 hours), medium term (6 hours to 1 day) and long-term (1 day to 1 week) wind forecasting [24]. Okumus et al. have reviewed recent forecasting schemes that include hybrid methods for improving the accuracy of prediction [25]. Among these the most used forecasting methods are a combination of two or more machine learning methods combined with a time-series model (ARMA and ARIMA). Further on the basis of time-series based forecasting models like that of Autoregressive Moving Average (ARMA), Autoregressive Integrated Moving Average

(ARIMA) methods are employed for short-term wind speed and power forecasts. Wind speed time-series poses non linearity in its nature which makes it difficult for statistical models to capture the trends. For the same reason, machine learning techniques like Artificial neural network, Support vector regression and Extreme learning machines are used [26]. The accuracy in wind speed prediction determines the dependency on the storage systems to outlay the economic blueprint for the entire system. Various hybrid techniques have been employed recently to study short-term wind forecasting for wind farms. Signal decomposition methods like wavelet transform and empirical mode decomposition are commonly used for studying the stochasticity in wind speed. Wavelet decomposition along with neural networks is studied by Du et al. and related works where the prediction accuracy has been enhanced with a multi-objective optimization of hyperparameters [27, 28, 29, 30, 31]. The model is then compared with benchmark methods like Persistence method, ARIMA and Generalized neural network. Results reveal that multi-objective optimization based neural network models outperform the benchmark model and are reliable for handling the short-term wind forecasting needs.

Forecasting wind speed in presence of wind wakes is an uphill task. Wind wakes cause reduction in power captured from wind resource, thus optimal placement of wind turbines in a farm will lead to efficient land area usage. In case of a wake affected downwind turbine, the most significant upwind turbines will affect the forecasting accuracy of the downwind turbine. Here, most significant upwind turbines refers to a set of turbines whose wake effect causes maximum power deficit at a downwind turbine. The major contributions of this paper are

1. A bilateral Gaussian wake model comprising Jensen and Frandsen component is proposed and is tested for single wake and multiple wake scenarios considering two artificial wind farm layouts for two wind speed datasets.
2. Short-term wind speed forecasting is studied considering the wake effects and significant upwind turbines are identified using Grey relational analysis. Forecasting accuracy is analyzed for proposed bilateral Gaussian wake model and benchmark models.

This paper is divided as follows. Section 2 describes various wind wake models, that is, Jensen's, Frandsen's and proposed bilateral Gaussian wake model. Section 3 discusses the individual methodologies for short-term wind speed forecasting in presence of wakes. In Section 4 results and in Section 5 discussions are presented followed by Conclusions in Section 6.

2. Wind Wakes

As discussed in previous section wind wakes lead to reduction in velocity at the downwind turbine in a wind farm. Wake affected wind turbine also suffers from the problem of increased mechanical loading on the turbine structure. Apart from analytical wake models cited in literature like Jensen's model, Ainslie's model, Larsen's model and Frandsen's model, many field models like 2D and 3D field models based on Computational Fluid Dynamics (CFD) have also been put into wake modeling. However due to computational uncertainly and time consumption analytical wake models are a preferred choice over field models [7]. We now discuss various analytical models for single wake and multiple wake conditions in a wind farm layout.

2.1. Jensen's and Frandsen's single wake model

N.O. Jensen [32] proposed a single wake model based on the assumption that the wake cone extends linearly with the downwind distance as shown in Figure 1. The free stream wind speed u_0 is an expected wind speed to be received by the downwind turbines, but due to wake effect a velocity deficit is observed at these turbines. Based on the conservation of momentum of fluid across the wake cone, the radius of wake affected wind turbine at a distance x from the upwind turbine can be expressed as

$$r_x = r_0 + \alpha x, \tag{1}$$

where r_0 is the rotor radius of the wind turbine, α represents the rate of wake expansion behind rotor and x is the downwind distance as shown in Figure. 1.

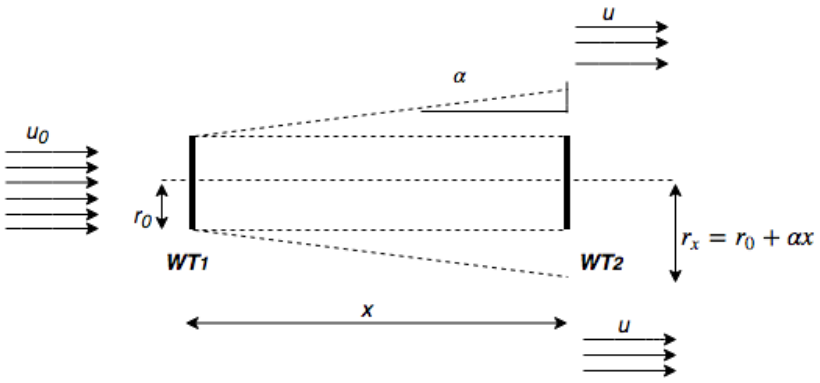

Figure 1: Wind turbine layout for Jensen's single wake model

The choice of value of α depends on the wind farm terrain (surface roughness, hub height) and atmospheric conditions (air turbulence). An empirical estimation of wake expansion constant α is

$$\alpha = \kappa \left[log_e\Big(\frac{h}{z_0}\Big) - \psi_m(h/L) \right]^{-1} \tag{2}$$

where $\kappa = 0.4$ is the von Karman constant, h, z_0 are the hub height of turbine and surface roughness length. The factor $\psi_m(h/L)$ determines the local atmospheric stability correction at a given hub height [33]. The effective wind u_j speed at the downwind turbine located at a distance x due to wake effect of a single upwind turbine as per Jensen's model is given as

$$u_j = u_0 \left(1 + (\sqrt{1 - C_t} - 1)\Big(\frac{r_0}{r_x}\Big)^2 \right), \tag{3}$$

where $C_t = a(2 - a)$ is the thrust coefficient with induction factor $a = 1 - \frac{u_j}{u_0}$ as per Actuator disk theory.

Frandsen et al. [7], have described the wake expansion immediately after rotor as rectangular profile compared to trapezoidal profile in Jensen's model. The wind speed u_f at a downwind distance x as per Frandsen's model is

$$u_f = u_0 \left(\frac{1}{2} \pm \frac{1}{2} \sqrt{1 - 2C_t \Big(\frac{r_0}{r_x}\Big)^2} \right). \tag{4}$$

An empirical result was obtained in order to estimate the relationship between r_x and C_t, α and r_0 which is given as

$$r_x = r_0(\beta + \alpha x/2r_0)^{1/2}, \tag{5}$$

$$\beta = 0.5\left(\frac{1+\sqrt{1-C_t}}{\sqrt{1-C_t}}\right). \tag{6}$$

In (4), the '+' sign is applicable for $a \leq 0.5$ and '$-$' sign for $a > 0.5$.

2.2. Proposed model for wind wakes

The velocity deficit estimated by Jensen and Frandsen are based on the top-hat like velocity distribution. Several wind tunnel experiments have shown that the velocity deficit in transverse direction for a far-wake region follows a Gaussian distribution [11]. Wu and Porté-Agel [34]. have studied turbulence effect on stand-alone turbine wakes based on large-eddy simulation (LES) framework. The velocity deficit at the far-wake end assumes a Gaussian distribution [35] such as

$$u = u_0\Big(1 - A(x)e^{\frac{-r^2}{2\sigma^2}}\Big), \tag{7}$$

$$A(x) = 1 - \sqrt{1 - \frac{C_t}{8(\sigma/2r_0)^2}} \tag{8}$$

where u_0 is the free-stream wind speed, $A(x)$ is the maximum normalized velocity deficit caused at each downstream position x and σ is the wake width for each downwind distance x.

However, the mass flow rate between the wind turbines is not constant as certain percent of incoming kinetic energy of wind is lost due to air turbulence. Another wake model proposed by Larsen was used to determine the speed of wind in wake affected area downstream but due to high computational requirements it is not preferred here. Based on the Gaussian variation of Jensen's and Frandsen's wake models, we propose a bilateral Gaussian wake model as shown in Figure 2 where two wind turbines are placed apart "x" rotor diameter and the velocity deficit assumes a Gaussian distribution at the far-end. The

wake expands linearly with downstream distance x and is dependent on atmospheric conditions in terms of stability factor measured by $\psi_m(h/L)$ and terrain conditions in terms of surface roughness length (z_0).

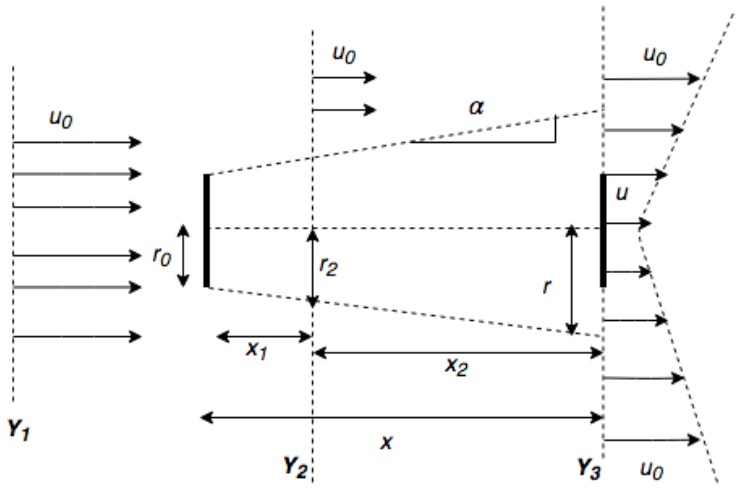

Figure 2: bilateral Gaussian wake model

Boundary lines Y_1, Y_2 and Y_3 are the regions where the wake effect is analyzed based on Jensen's and Frandsen's original wake scenario. According to Jensen, in the boundary Y_2 and Y_3, the law of conservation of mass holds true which can be mathematically expressed as:

$$\int_{r_2}^{\infty} \rho u_0 2\pi r dr + \int_0^{r_2} \rho u_2 2\pi r dr = \int_0^{\infty} \rho u 2\pi r dr, \tag{9}$$

$$u_2 = (1-2a)u_0, \tag{10}$$

where r_2 is the radial distance from wake centerline at downstream distance x_1, ρ is the density of incompressible fluid (here air), u_2 is the wind speed just after the rotor. According to actuator disk theory, u_2 is related to u_0 as (10), where a is the induction factor. Substituting (10) and (7) in (9), we get

$$A(x) = \frac{a}{(\sigma/r_2^2)} \tag{11}$$

where σ is a linear function of downstream distance x and its estimation [36] is

$$\sigma = \frac{r}{\sqrt{2}} = \frac{r_0 + \alpha x}{\sqrt{2}}, \tag{12}$$

Thus Jensen's gaussian distribution wake model is given as

$$u = u_0\left(1 - \frac{a}{(\sigma/r_2^2)}e^{\frac{-r^2}{2\sigma^2}}\right). \tag{13}$$

Further, Frandsen's Gaussian version of wake model assumes that mass flow rate through the control tube Y_1Y_3 is not constant. Based on the conservation of momentum,

$$T = \int_0^\infty \rho(u_0 - u)2\pi r dr = \frac{1}{2}\rho A_0(u_0^2 - u^2), \tag{14}$$

where T is the net thrust in presence of wake flow speed u. Further, substituting (11) and (7) in (14), we get

$$A(x) = 1 - \sqrt{\left(1 - \frac{C_t}{2(\sigma/r_0)^2}\right)}, \tag{15}$$

$$\sigma = \frac{r}{2} = \frac{r_0 + \alpha x}{2}, \tag{16}$$

where $A(x)$ is the maximum normalized velocity deficit caused in wakes, σ is the wake width for a given downstream distance x. We now propose a bilateral Gaussian wake model based on Jensen's and Frandsen's Gaussian wake approach, mathematically it can be expressed as

$$u = u_0\Big(1 - Q(x,r)\Big), \tag{17}$$

$$Q(x,r) = A_j(x,r)A_f(x,r), \tag{18}$$

$$\sigma_j = \frac{r_0 + \alpha x}{\sqrt{2}}, \quad \sigma_f = \frac{r_0 + \alpha x}{2}, \tag{19}$$

$$A_j(x,r) = \frac{a}{(\sigma_j/r_2^2)}e^{\frac{-r^2}{2\sigma_j^2}}, \tag{20}$$

$$A_f(x,r) = \left(1 - \sqrt{\Big(1 - \frac{C_t}{2(\sigma_f/r_0)^2}\Big)}\right)e^{\frac{-r^2}{2\sigma_f^2}}$$

where $A_j(x,r)$ and $A_f(x,r)$ are the respective Jensen and Frandsen Gaussian components for a given downstream distance x and radial distance r which is a function of wake expansion factor α and downstream distance x. Further σ_j and σ_f are the wake width as a function of x for Jensen and Frandsen

model respectively. The motivation behind multiplying Jensen's ($A_j(x,r)$) and Frandsen's ($A_f(x,r)$) component comes from the individual advantages of the two models. Jensen's model is time-saving whereas Frandsen's model holds good approximation for far-wake region ($5D_0-7D_0$). The proposed bilateral Gaussian wake model was tested against benchmark Jensen's and Frandsen's wake model for single wake and multiple wake scenario and its results are presented in next subsection. In case of our proposed model the wake velocity u is calculated for a fixed radial distance for a given wake expansion factor α as listed in Table 1.

Table 1: Turbine specifications for wake model calculation

Parameter	Value
Rotor radius (r_0)	38.5 m
Thrust coefficient (C_t)	0.88
Wake constant (α)	0.05
Hub height (h)	61 m

2.3. Case study for single wake model

In this paper, two analytical models, that is, Jensen's and Frandsen's single wake model are discussed. In order to analyze the performance of these individual models, the wind speed data for a wind site WBZ (earlier known as Westinghouse Broadcasting,radio station in Boston) Tower Hull located in Boston Harbor, Massachusetts is collected from September 1, 2006 to September 30, 2006. Wind speed was measured every 10 minutes at a hub height of 61 meters by a cup anemometer with an accuracy of $\pm 2\%$. The wind speed series chosen for 250 data points has maximum and minimum wind speed of 13.05 m/s and 1.5 m/s respectively and a mean wind speed of 7.58 m/s. The wake growth constant (α) is calculated using empirical relationship (2) for given hub height (h) and surface roughness length (z_0). Since the wake effect is analyzed in neutral atmospheric boundary layer, the atmospheric stability correction factor ($\psi_m(h/L)$) is considered zero. Similarly, for C_t, the value 0.88 is chosen based on the assumption that every turbine in a wind farm is operating at Betz limit

where the coefficient of power is 0.58, which occurs at a =0.33, where a is induction factor. For a neutral atmospheric boundary layer (ABL) operation the value of C_t is found to be higher for increased power output [37]. The wake flow behind the upwind turbine is dependent on the wake growth constant α and that in turn depends on the topographical features (surface roughness length) of the wind farm land.

Consider a single wake wind turbine layout in Figure 1. Wind turbine 1 (WT_1) is upwind turbine and wind turbine 2 (WT_2) is downwind turbine. The wind speed for WBZ tower Hull varies in the range of 1.5 m/s to 13.05 m/s, given that the ABL is not stratified (density variation of air in vertical direction is zero) pressure drop at hub of each wind turbine in the farm is constant, the thrust coefficient (C_t) remains constant for wake stream flow. The effective wind speed observed is simulated using (3) and (4) and Root Mean Square Error (RMSE) and Coefficient of determination (R^2) were calculated to assess the model performance for a single wake model. Table 2 depicts performance metrics and Frandsen's single wake model outperforms Jensen's model in terms of RMSE and R^2. The proposed and benchmark models are tested for different downwind distances ($x = 2.5D_0, 3D_0$ and $5D_0$).

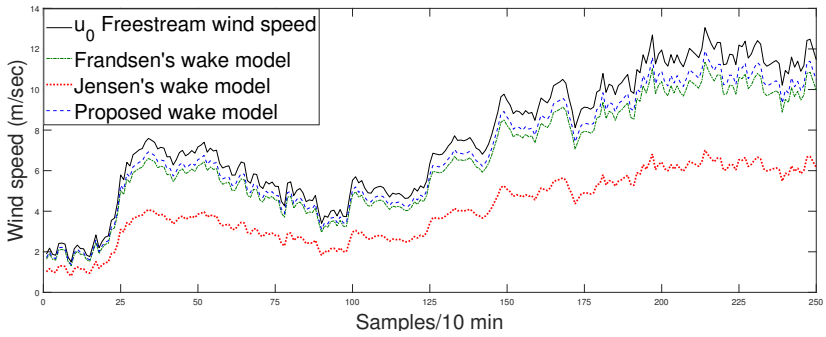

Figure 3: Wake effect on WT_2 due to WT_1 based on benchmark models and proposed model.

Figure 3 shows the effective wind speed observed at wind turbine WT_2 due to wake effect of WT_1 for Jensen', Frandsen's and proposed bilateral Gaussian wake model for a downwind distance of $2.5D_0$ and u_0 refers to the freestream

Table 2: Performance indices for single wake scenario

Model	Metric	$2.5D_0$	$3D_0$	$5D_0$
Jensen	RMSE	3.7865	3.5461	2.7769
	R^2	0.8628	0.8683	0.8605
Frandsen	RMSE	1.0668	0.9375	2.7769
	R^2	0.8885	0.8780	0.8964
Proposed	RMSE	0.7148	0.7146	0.7169
	R^2	0.8976	0.8823	0.8971

wind speed. Based on root mean squared error (RMSE), the proposed bilateral Gaussian wake model outperforms Jensen's model by 81.11% and Frandsen's model by 32.99% for a downstream distance of $2.5D_0$.

2.4. Multiple wake model

This study can be further extended for wind wakes due to multiple upwind turbines. Due to shadowing effect created by wind turbines placed at different locations, the effective wind speed in presence of wakes using Jensen's model [38] is

$$u = u_0\left(1 - \sum_{i=1}^{N}\left(1 - \sqrt{1-C_t}\Big(\frac{r_0}{r_{ij}}\Big)^2 \frac{A_{sh,i}}{A_0}\right)\right), \tag{21}$$

where $A_{sh,i}$ is the overlap area experienced by wind turbine under shadow from upwind turbine, and

$$\begin{aligned} A_{sh,i} \quad = \quad & r_0^2 \cos^{-1}\left(\frac{d_{ij}^2 + r_0^2 - r_{ij}^2}{2d_{ij}r_0}\right) + r_{ij}^2 \cos^{-1}\left(\frac{d_{ij}^2 + r_{ij}^2 - r_0^2}{2d_{ij}r_{ij}}\right) \\ & -\frac{1}{2}\sqrt{\Big((r_0 + d_{ij})^2 - r_{ij}^2)(r_{ij}^2 - (r_0 - d_{ij})^2\Big)} \end{aligned} \tag{22}$$

and based on Frandsen's wake model the effective wind speed during multiple wake scenario is given as

$$u = u_0\left(\frac{1}{2} \pm \frac{1}{2}\sqrt{1 - 2C_t\Big(\frac{r_0}{r_{ij}}\Big)^2\left(\frac{A_{sh,i}}{A_0}\right)}\right), \tag{23}$$

where d_{ij}, r_0, r_{ij} are the horizontal distances between upwind turbine WT_i and downwind turbine WT_j, rotor radius for all turbines in wind farm, radius of the downwind turbine WT_j due to wake effect of WT_i and N are the total number of wind turbines causing shadowing effect.

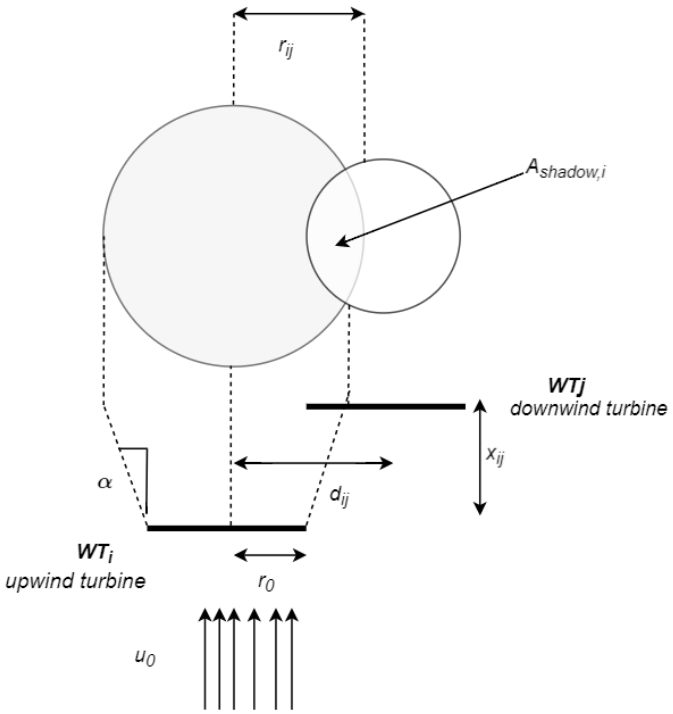

Figure 4: Shadowing effect in case of multiple wake scenario

Figure 4 shows the overlap area experienced by downwind turbine. Based on the overlap area, the degree of shadowing is calculated for multiple wake scenario where a wind turbine receives wind wakes from more than one upwind turbine. For our proposed bilateral gaussian wake model, the effective wind speed at WT_j due to N upwind turbines WT_i, where $(i = 1, 2, \ldots, N)$ is given as

$$u = u_0\Big(1 - \sum_{i=1}^{N} Q_{ij}(x, r)\Big), \tag{24}$$

$$Q_{ij}(x, r) = A_{ij}(j)A_{ij}(f)D_{o,i},$$

$$D_{o,i} = \Big(\frac{A_{sh,i}}{A_0}\Big), \tag{25}$$

where N are the total number of upwind turbines causing shadowing on downwind turbine WT_j, $D_{o,i}$ is the degree of overlap due to shadowing, $A_{ij}(j)$ and $A_{ij}(f)$ are the Jensen and Frandsen component calculated using (20). To test Jensen's and Frandsen's model for multiple wake condition, a 5 turbine Wind Farm Layout (WFL) is chosen in Figure 5. In order to study the multiple wake effect following assumptions were made:

A1 All the wind turbines in the wind farm have same rotor diameter D_0.

A2 After a downwind distance of $10D_0 - 12D_0$ the wake effect due to wind turbine WT_1 disappears.

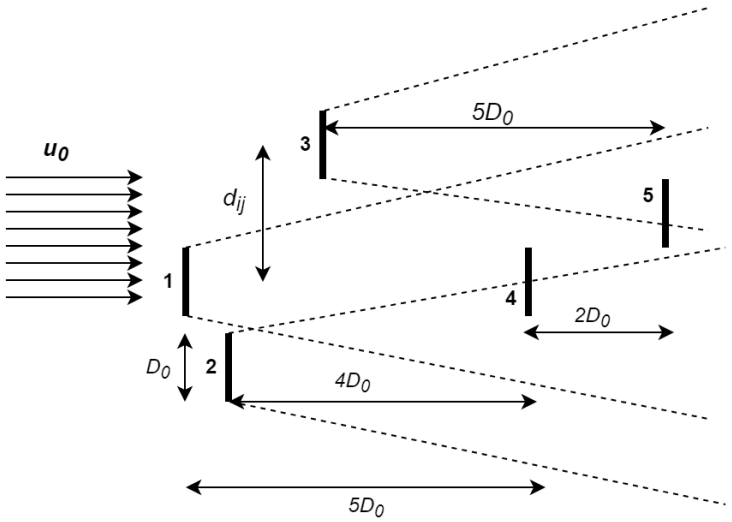

Figure 5: Wind farm layout consisting 5 wind turbines

The multiple wake condition based on Jensen's model and Frandsen's model is tested on a 5 wind turbine layout as shown in Figure 5. The effective wind speed observed at WT_4 and WT_5 due to multiple upwind turbines are calculated using (21) and (23). The effective wind speed at WT_4 and WT_5 due to multiple wake effect is shown in Figure 6.

From Figure 6 we can observe that Frandsen's model for multiple wake outperforms Jensen's model. Further, as the distance x_{ij} between upwind and

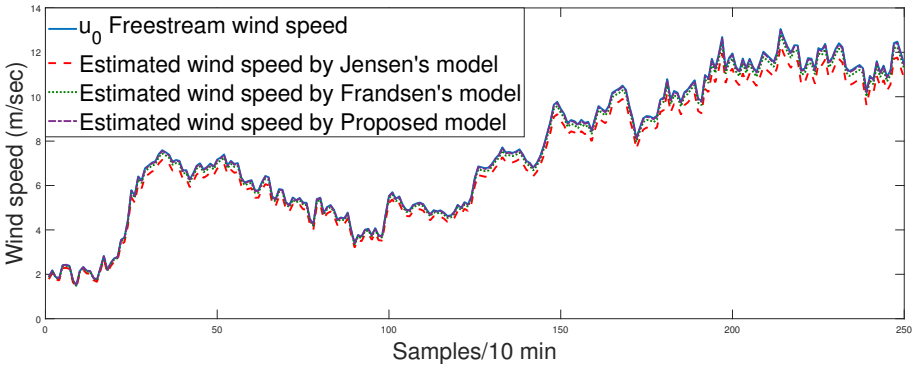

Figure 6: Effective wind speed at WT_4 due to wake effect of WT_1 and WT_2

downwind turbines increases, the wake effect diminishes. The performance of Jensen's and Frandsen's model multiple wake conditions is tested for wind turbines WT_4 and WT_5 for a 5-turbine wind farm layout.

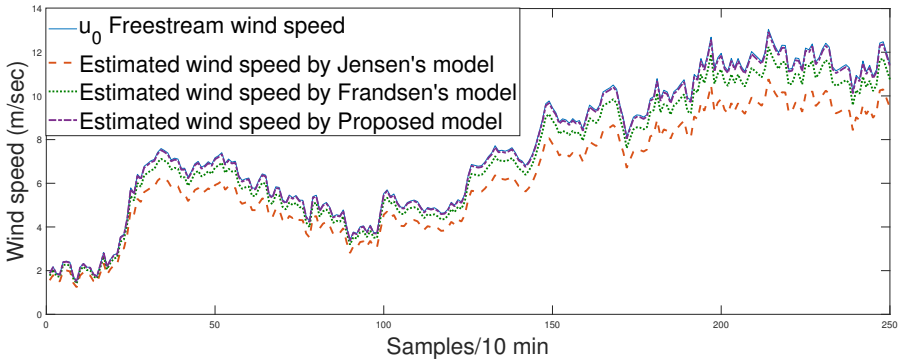

Figure 7: Effective wind speed at WT_5 due to wake effect of WT_1,WT_3 and WT_4

The performance metric, that is, RMSE for the benchmark models and proposed model was evaluated. For WT_4, the RMSE is found to be 46.70% using Jensen's model and 15.88% using Frandsen's model. Similarly for WT_5, the RMSE based on Jensen's model is 142.91% and based on Frandsen's model it is 50.81%. Compared to benchmark models the RMSE values based on proposed model for WT_4 and WT_5 are found to be 3.85% and 7.56% respectively. The velocity distribution at the far-wake end complies well with experimental results [39].

Further, the proposed wake model is validated by testing for multiple wake scenario for a dataset D2. The wind speed data is obtained for a wind farm Sotavento, Spain. Hourly wind speed data was measured from March 1, 2018 to March 30, 2018 by a cup anemometer placed at a height of 61 meters. Out of this dataset, first 250 data points are chosen for testing multiple wake scenario. The descriptive statistics for dataset D2 are u_{max}= 17.3 m/s, u_{min}= 0.35 m/s, u_{mean}=7.625 m/s and standard deviation of 2.677. For wind turbine WT_4, RMSE is found to be 33.87% using Jensen's model, 11.72% using Frandsen's model and 2.344% using proposed model. For wind turbine WT_5, the RMSE for Jensen's model is 111.44% and 39.2% using Frandsen's model. Compared to benchmark model the proposed model recorded RMSE of 4.2%. Figure 8 shows the wake velocity for WT_4 and WT_5 based on Jensen's , Frandsen's and Proposed wake model.

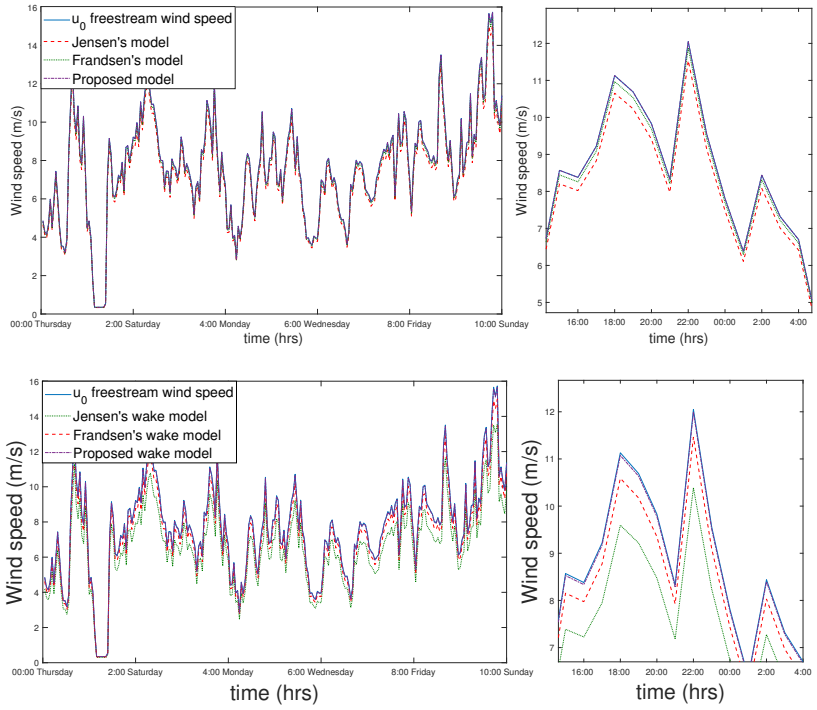

Figure 8: Effective wind speed at WT_4 and WT_5 due to wake effect of (WT_1,WT_2) and (WT_1,WT_3 and WT_4) for dataset D2

3. Wind forecasting considering wake effect

Wind forecasting is an essential step in terms of planning and operating a wind farm which is tied to a utility grid. Various methods based on time-series method like Auto regressive Integrated Moving Average (ARIMA) and intelligent learning algorithms like Artificial Neural Networks (ANN) and Support Vector Regression (SVR) are preferred for wind forecasting [40]. Here we study the forecasting in presence of wind wakes. In a particular wind farm, not all wind turbines receive the wind speed at same magnitude and direction. Also for a multiple wake condition, a wind turbine experiences wake due to multiple upwind turbines but not all wind turbines cause significant wake effect and turbulence on the downwind turbine. Since not all upwind turbines cause velocity deficit, to identify the significant upwind turbines on a particular downwind turbine, Grey Correlation Analysis (GRA) is performed. The following subsection discusses the various steps involved in Grey correlation analysis.

3.1. Grey correlation analysis

Grey correlation analysis or grey relational analysis (GRA) is an important financial tool often used in system analysis technique [41]. The central idea of GRA is to establish degree of closeness among various decision making sequences and a reference sequence. The forecasting accuracy considering wake effects from multiple upwind turbines is greatly affected by the results of GRA. Further, once the GRA is done, only those variables which have higher grey correlation degrees are chosen as inputs for the wind speed forecasting model. Grey correlation analysis is done as follows:

1. A reference sequence with length same as that of decision making sequences is chosen as $X_0 = (x_{01}, x_{02}, \ldots, x_{0n})$, and decision sequences are expressed as a matrix L representing all the decision sequences along

with the reference sequence X_0, where $X_i = (x_{i1}, x_{i2}, \ldots, x_{in})$, where $i = 1, 2, \ldots, m$.

$$L = \begin{bmatrix} x_{01} & x_{11} & \ldots & x_{m1} \\ x_{02} & x_{12} & \ldots & x_{m2} \\ \vdots & \vdots & \ddots & \vdots \\ x_{0n} & x_{1n} & \ldots & x_{mn} \end{bmatrix}. \tag{26}$$

2. Next, all the sequences are standardized either through transforms such as initial value transform, average value transform or polar difference transform. After this procedure, the matrix L is transformed as

$$L^{'} = \begin{bmatrix} x_{01}^{'} & x_{11}^{'} & \ldots & x_{m1}^{'} \\ x_{02}^{'} & x_{12}^{'} & \ldots^{'} & x_{m2}^{'} \\ \vdots & \vdots & \ddots & \vdots \\ x_{0n}^{'} & x_{1n}^{'} & \ldots & x_{mn}^{'} \end{bmatrix} \tag{27}$$

3. After standardization, calculate the absolute difference of the corresponding elements of reference sequence and decision sequence, i.e., $\Delta_{ik} = |x_{0t}^{'} - x_{ik}^{'}|$, where $i = 1, 2, \ldots, n$ and $k = 1, 2, \ldots, m$.

4. Calculate $gg = min(\Delta_{ik})$ and $hh = max(\Delta_{ik})$.

5. Compute relational coefficient between reference sequence $x_{0t}^{'}$ and decision sequence $x_{it}^{'}$ using

$$r(x_{0t}^{'}, x_{it}^{'}) = \frac{gg + \rho \times hh}{\Delta_{it} + \rho \times hh} \tag{28}$$

where $\rho \in (0, 1)$ is called the distinguish coefficient. Usually $\rho = 0.5$ is taken for all the calculations.

6. Compute the grey relational degree using following equation

$$r(X_0, X_i) = \frac{1}{n} \sum_{i=1}^{n} r(x_{0t}^{'}, x_{it}^{'}), \quad i = 1, 2, \ldots, m. \tag{29}$$

7. The grey relational degree is ordered in descending order and the first j^{th} inputs are selected for forecasting wind speed in presence of wakes.

In this study, Grey relational analysis is used to identify the upwind turbines that significantly affect the given downwind turbine. The wake wind speed due to individual upwind turbine is treated as decision sequence and freestream wind speed u_0 is treated as reference sequence X_0. The short-term wind speed forecasting is carried without GRA and with GRA and the forecasting results in terms of RMSE are then compared for the proposed bilateral Gaussian wake model and benchmark models.

3.2. Wavelet-Support vector regression for wind forecasting

Wind forecasting is primarily done by forecasting wind speed or wind power. Recently machine intelligent algorithms like Artificial neural networks (ANN), Support vector regression (SVR) [42] and Extended learning machine (ELM) [43] are used for wind forecasting. Further hybrid methods that involve decomposition methods (Wavelet transform, Empirical mode decomposition) are also used in combination with individual methods to obtain better forecast accuracy [44]. Liu et al. [45] have proposed an improved SVM method for wind forecasting by optimizing hyperparameters by using simulated annealing (SA). Here to forecast wind speed in presence of wakes we use a hybrid method based on wavelet-SVR. Firstly, the wavelet transform filters the wind speed time-series from potential stochastic variations, then the inputs to the SVR model are chosen based on Grey correlation analysis. The forecasted wind speed is then compared with actual wind speed and various performance indices are computed to evaluate forecasting model.

Introduced by Moret et al., Wavelet transform was first put into use for analyzing seismic waves [46]. Wavelet transform is a multi-resolution method used to fragment a signal into subsequent approximate (low frequency) and detail (high frequency) components. The wavelet transform for an input signal $z(t)$ is given as

$$W(p_z, q_z) \quad = \quad 2^{-p_z/2} \sum_{t=0}^{N-1} z(t)\phi\left(\frac{t - q_z.2^{p_z}}{2^{p_z}}\right), \tag{30}$$

where N represents the signal length, scaling and translation parameters are the functions of p_z and q_z which are integers. $\phi(t)$ is chosen as mother wavelet. Daubechies (db4) wavelet transform is applied to the wind series. A 5-level signal decomposition is done and its results are shown in Figure 9 with five detail signals and one approximate signal (a5) which are used as input feature set for short-term wind forecasting in presence of wind wakes.

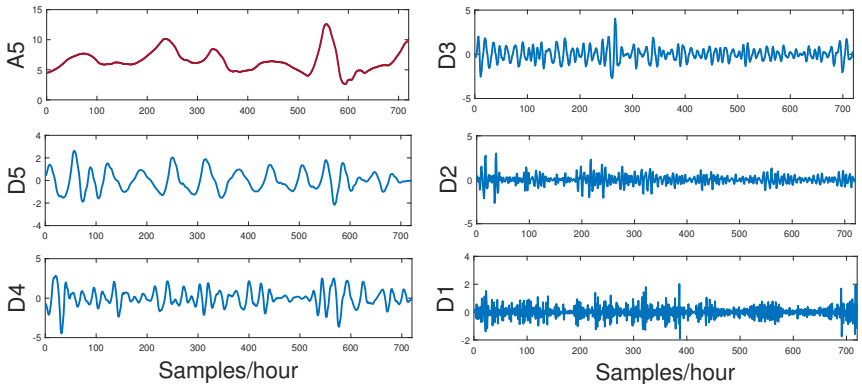

Figure 9: 5-level db4 wavelet decomposition for wind speed time series

Support vector regression is a machine learning algorithm developed by Vapnik [47]. The idea of support vector regression using Support vector machine (SVM) is based on structural risk minimization theory. Consider input-output pair (x_i, y_i), where $x_i \in \mathrm{X}$, $\mathrm{X} \in \mathrm{R^n}$ and $y \in \mathrm{R}$. Here x_i for $i = 1, 2, \ldots, n$ are the set of features that are taken as input for the SVR model. The SVR problem is based on convex optimization of a risk functional represented by a linear regressor

$$f_{SVR}(x) = w^T x + b, \text{with } w \in \mathrm{X}, b \in \mathrm{R}, \tag{31}$$

where x is the input feature set, w is the weight coefficient vector and b is the bias term correction, and can be expressed as a minimization problem

$$\min \frac{1}{2} \parallel w \parallel^2 + \gamma(e^T\xi + e^T\xi^*), \tag{32}$$

$$\text{subject to } \; y - w^T x - eb \leq e\varepsilon + \xi, \xi \geq 0, \tag{33}$$

$$w^T x + eb - y \leq e\varepsilon + \xi^*, \xi^* \geq 0,$$

where γ is the regularization factor that trade-offs the flatness of regressor $f_{SVR}(x)$ and the maximum acceptable deviation ε. The variables ξ, ξ^* are the slack variables introduced as a soft margin to the acceptable error ε and e is the vector of ones of appropriate dimensions. For non-linear regression problems, kernel functions which satisfy Mercer's theorem such that $k(x_i, x_j) = \langle \phi(x_i), \phi(x_j) \rangle$, where K denotes the kernel matrix with elements $K_{ij} = k(x_i, x_j)$ are used. In its dual form, the SVR problem may be extended as

$$\min \frac{1}{2} \sum_{i,j=1}^{n} (\chi_i - \chi_i^*)^T k(x_i, x_j)(\chi_j - \chi_j^*) + e^T \varepsilon \sum_{i=1}^{n} (\chi + \chi^*) - \sum_{i=1}^{n} y_i(\chi - \chi^*),$$
$$\textbf{s.t.} \quad e^T \sum_{i=1}^{n} (\chi_i - \chi_i^*) = 0, \quad 0 \leq \chi, \quad \chi^* \leq \gamma e, \tag{34}$$

where χ and χ^* are the Lagrange multipliers such that $\chi_i \chi_i^* = 0$, $i = 1, 2, \ldots, n$. The regressor $f_{SVR}(x)$ is given as

$$f_{SVR}(x) = \sum_{i=1}^{n} (\chi_i - \chi_i^*) k(x_i, x) + b. \tag{35}$$

4. Results

This section throws light on the framework for short-term forecasting in presence of wind wakes for two wind farm layouts, that is, 5-turbine wind farm layout (Figure 3) and 15-turbine wind farm layout (Figure 13). Wind speed data is collected for two data sets a wind farm WBZ tower Hull, Boston Harbor, Massachusetts and another one located in Sotavento, Galicia, Spain. Table 3 shows the descriptive statistics for the two wind farms with their sampling time.

Table 3: Descriptive statistics for wind speed for WBZ tower Hull, MA and Sotavento, Spain

Wind Farm	Dataset	Max (m/s)	Min (m/s)	Mean (m/s)	Std Dev
WBZ tower, MA	D1	10.14	0.36	4.4966	2.3143
Sotavento, Spain	D2	17.53	0.35	7.1768	2.8009

Figure 10 shows the wind speed time-series for the two wind farms WBZ tower Hull and Sotavento, Galicia. Each of the two datasets D1 and D2 have

different sizes 500 data points and 720 data points respectively. The data points for dataset D1 were obtained at every 10 minute and for dataset D2 the points were obtained at every hour from March 1, 2018 00:00 hrs (GMT) to March 30, 2018 00:00 hrs (GMT), that is, 24 observations each day and 720 observations for the entire month.

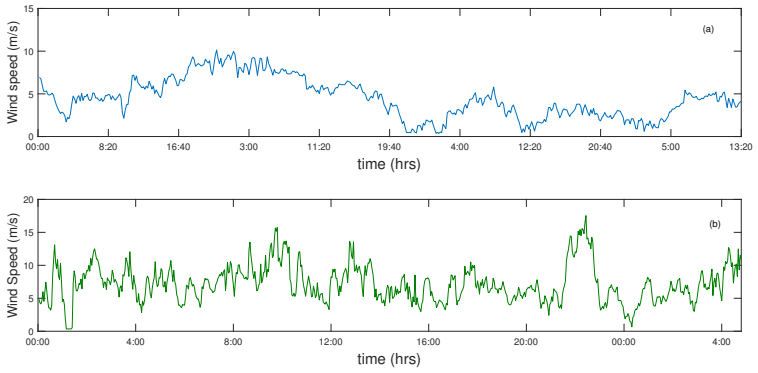

Figure 10: Wind speed time-series (a) WBZ tower Hull, MA (b) Sotavento, Galicia, Spain.

The short-term wind speed forecasting, that is (10 minutes for D1) and 1 hour(for D2), is analyzed on the basis of standard metrics like Root mean squared error (RMSE), Sum of squared residuals (SSR) and Sum of squared deviation of testing samples (SST). Mathematical expressions for these metrics are

$$\begin{aligned} \text{RMSE} &= \sqrt{\frac{1}{N}\sum_{i=1}^{N}(\hat{X}_i - X_i)^2} \times 100\% \\ \text{SSR/SST} &= \frac{\sum_{i=1}^{N}(\hat{X}_i - \bar{X})^2}{\sum_{i=1}^{N}(X_i - \bar{X}_i)^2} \end{aligned} \tag{36}$$

where $\hat{X}_i, X_i, \bar{X}$ are the predicted, actual and mean values of the N testing samples. Lower the RMSE and value better the forecasting model. A high SSR/SST ratio indicates a good agreement between actual and estimated values of testing samples.

4.1. Forecasting results for 5-turbine wind farm layout

The forecasting process involves first calculating wind speed received by the downwind turbine under wake effect from individual upwind turbines. The wind

farm layouts for 5-turbine wind farm and 15-turbine farm are selected. In case of wind farm layout with 5 turbines, wind farms WT_4 and WT_5 are the downwind turbines. The wake flow speed for both the wind turbines is calculated using Jensen's and Frandsen's model. The turbine parameters for both the wind farm layouts are chosen same for simplicity, and are listed in Table 1. Wind turbine WT_4 experiences wake from WT_1 and WT_2, whereas wind WT_5 experiences wake from WT_1, WT_3 and WT_4. The distance x_{ij} between upwind (WT_i) and downwind turbines (WT_j) is listed in Section 2.4. After calculation of wake flow speed using (3) and (4), the wake flow speed time-series is analyzed for grey correlation analysis by comparing it with a reference sequence X_0 (freestream wind speed u_0 here). The grey correlation degree (GCD) $r(u_0, u_{ij})$ obtained thereafter is arranged in descending order of its magnitude and first j^{th}. In case of 5-turbine layout the GCD was found for wind speed series u_{15}, u_{35} and u_{45} to select inputs for forecasting wind speed for turbine WT_5. The Grey correlation analysis results for u_{15}, u_{35} and u_{45} are highlighted in Table 4.

Table 4: Grey correlation degree and its ranking for 5-turbine layout for dataset D1 and D2

Grey correlation degree	D1		D2	
	Value	Rank	Value	Rank
$r(u_0, u_{15})$	0.7074	3	0.5867	3
$r(u_0, u_{35})$	0.8529	1	0.6748	1
$r(u_0, u_{45})$	0.8234	2	0.5940	2

The GCD in descending order is $r(u_0, u_{35}) > r(u_0, u_{45}) > r(u_0, u_{15})$. Thus, we select u_{35} and u_{45} as inputs to the SVR model to forecast wind speed for turbine WT_5. Further the wind speed for turbine WT_5 is also forecasted without considering grey correlation analysis, that is, selecting all the wake causing wind turbines as input to the SVR model. The effective wind speed is decomposed into approximate signal (a5) and detail signals (d1, d2, d3, d4, d5) using 5-level daubechies 4(db4) wavelet transform. The forecasting is done using SVR model where the data is divided as training set (first 80%) and testing set (remaining 20%). The SVR model uses Radial Basis Function (RBF) as kernel

function. The SVR hyperparameters are chosen from the set $2^i|i = -9, -8, ...10$. This choice of search space enables one to determine optimal parameters from finite set of real numbers and leads to fast computation. We selected RBF kernel function for SVR forecasting and its bandwidth chosen was $\sigma = 2^5$ and regularization constant γ was taken as 2^2 [48]. Tables 5 shows the forecasting results for wind turbine WT_5 based on Jensen's and Frandsen's wake model for the two datasets D1 and D2.

Table 5: Forecasting results for wind turbine WT_5 for dataset D1 and D2

Dataset	Metric	Jensen's model	
		without GRA	with GRA
D1	RMSE (%)	6.53	5.84
	SSR/SST	1.0897	1.0124
D2	RMSE (%)	12.93	11.86
	SSR/SST	1.0483	1.0488
		Frandsen's model	
		without GRA	with GRA
D1	RMSE (%)	3.68	3.31
	SSR/SST	1.0986	1.0928
D2	RMSE (%)	9.02	6.43
	SSR/SST	1.0552	1.0578
		Proposed model	
		without GRA	with GRA
D1	RMSE (%)	2.86	2.56
	SSR/SST	1.1087	1.1902
D2	RMSE (%)	7.33	4.91
	SSR/SST	1.0270	1.0020

From Table 5, we find that wind forecast accuracy for Frandsen's model outperforms Jensen's model. Using our proposed model, short-term wind forecasting is carried out for datasets D1 and D2 and results are studied with respect to benchmark models. For dataset D1, the RMSE is found to be less than than

Jensen's and Frandsen's model. For dataset D1, without GRA, the RMSE is 2.86%, and for dataset D2, the RMSE is 7.33%. For dataset D1, the RMSE value without GRA based Jensen's model is 6.53% and based on Frandsen's model is 3.68%. The SSR/ SST ratio for Jensen's model is 1.0897 and using Frandsen's model is 1.0986. Further by incorporating GRA in our forecasting model, the RMSE for Frandsen's model is 3.31% and for Jensen's model it is 5.84%. The SSR/SST ratio for Frandsen's model is found to be better than Jensen's model thus suggesting better wind speed forecasting based on this model. A high SSR/SST ratio implies good agreement between actual and estimated values.

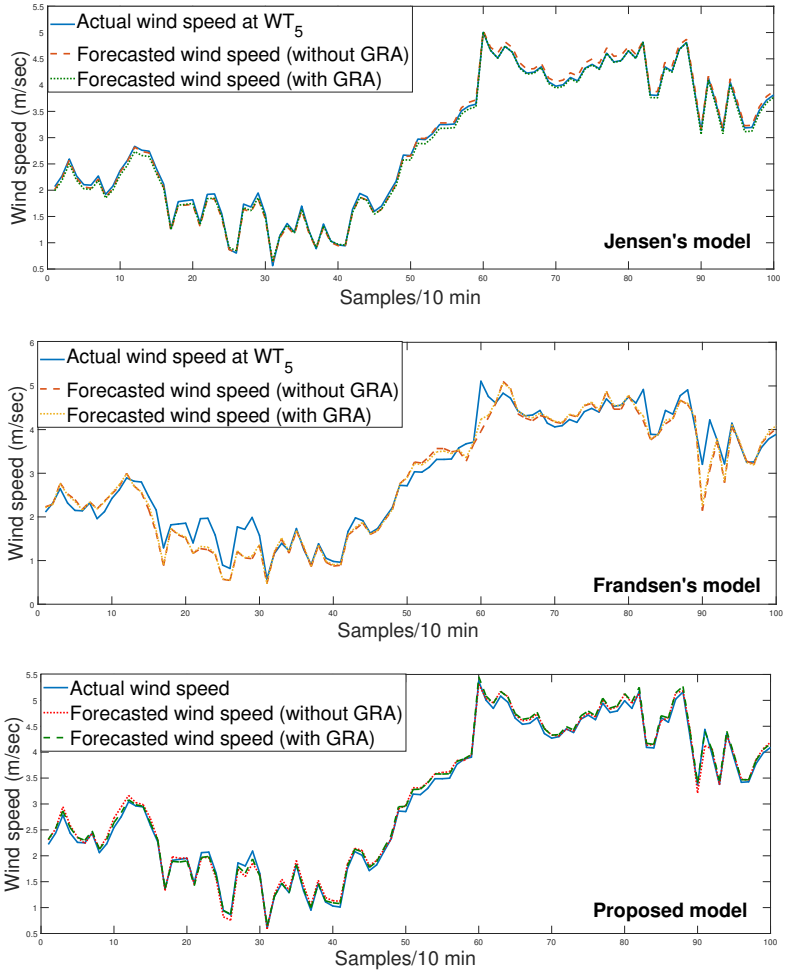

Figure 11: Wind forecasting for WT_5 with and without GRA for dataset D1.

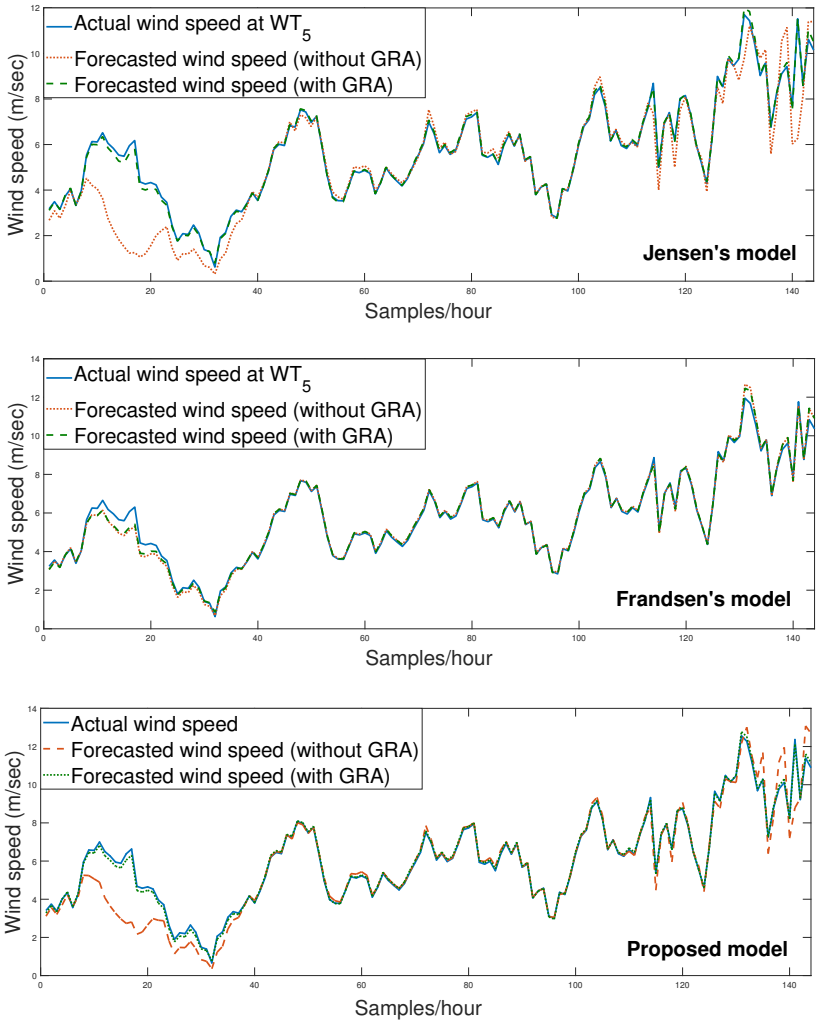

Figure 12: Wind forecasting for WT_5 with and without GRA for dataset D2.

Similarly for dataset D2, the effective wind speed for wind turbine WT_5 is calculated based on Jensen's and Frandsen's model and GRA analysis is done. Here the Grey correlation analysis results for u_{15}, u_{35} and u_{45}. Based on the GCD rankings we select u_{35} as the input to the SVR model along with decomposition signals using wavelet transform. The RMSE values for dataset D2 without GRA based on Jensen's model is 12.93% and based on Frandsen's model is 9.02%. The SSR/SST ratio for Jensen's model is 1.0483 and using

Frandsen's model is 1.0552. A high SSR/SST ratio implies that the regressor extracts maximum statistical information from the data. A wake model estimating lower velocity deficit yields higher Annual Electricity Production (AEP), thus ensuring better wind speed forecast and reliability.

Figures 11-12 show the short-term wind speed forecasting results for WT_5 in presence of wakes based on Jensen's, Frandsen's and proposed model for datasets D1 and D2 respectively. The short-term forecast was done using hybrid method wavelet-SVR for which 80% (400 data points) of data was used for training and 20% (100 data points) for testing.

4.2. Forecasting results for 15-turbine wind farm layout

Next, we discuss short-term wind speed forecasting in presence of wind wakes for a 15-turbine wind farm layout with turbines arranged asymmetrically as in Figure 13.

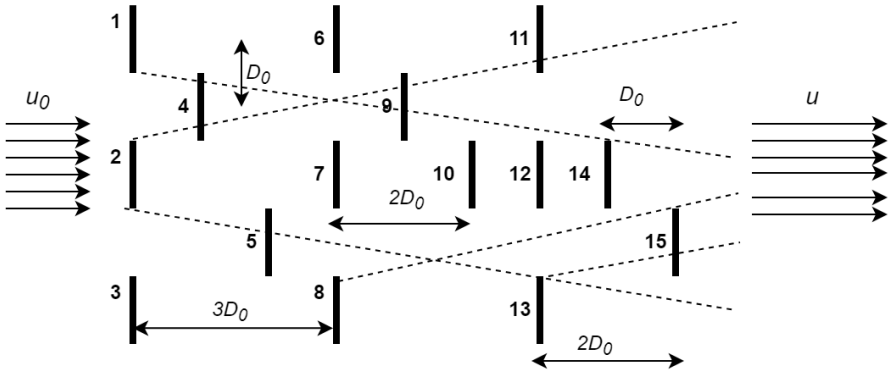

Figure 13: Schematic for a 15-turbine wind farm layout.

The wind turbine WT_{12} is affected from wakes by upwind turbines WT_3, WT_4, WT_5, WT_7, WT_9 and WT_{10}. The effective wind speed due to upwind turbines is calculated using (21) and (23) for Jensen's and Frandsen's model respectively.

$$u_{12eff} = u_0\left(1 - \sum_{i=1}^{N}\left(1 - \sqrt{1 - C_t}\left(\frac{r_0}{r_{ij}}\right)^2 \frac{A_{sh,i}}{A_0}\right)\right), \tag{37}$$

where u_{12eff} is the effective wind speed at WT_{12} due to wake effects of upwind turbines. The overlap area $A_{sh,i}$ due to upwind turbine WT_i is calculated using

(22). The wind speed series $u_{i,j}$ due to upwind turbine WT_i, $i = 3, 4, 5, 7, 9, 10$, based on Jensen's, Frandsen's and proposed model, is calculated. In Table 6, we calculate the Grey correlation degree $r(u_0, u_{i,j})$, with u_0 (freestream wind speed) as reference, using GRA for dataset D1 (WBZ tower Hull, Boston, MA) and dataset D2 (Sotavento, Galicia).

Table 6: Grey correlation degree and its ranking for 12-turbine layout for datasets D1 and D2

Grey correlation degree	D1		D2	
	Value	Rank	Value	Rank
$r(u_0, u_{3,12})$	0.8218	3	0.6644	5
$r(u_0, u_{4,12})$	0.8529	1	0.6748	4
$r(u_0, u_{5,12})$	0.7809	5	0.7065	3
$r(u_0, u_{7,12})$	0.7228	6	0.8246	1
$r(u_0, u_{9,12})$	0.8234	2	0.5940	6
$r(u_0, u_{10,12})$	0.7917	4	0.7260	2

The SVR model is trained for 80% of the data and tested for remaining 20% of data. RBF kernel function with bandwidth ($\sigma = 2^5$) is used. For dataset D1, the inputs to the SVR model are wavelet decomposition signals of effective wind speed u_{12eff} (a5; d1, d2, d3, d4 and d5) and wind speed series u_{ij} due to upwind turbines WT_i, where ($i = 3, 4, 5, 7, 9, 10$).

The short-term wind speed is forecasted for turbine WT_{12} once without GRA analysis, that is, all the inputs and once with GRA analysis, that is, only selected inputs ($u_{5,12}; u_{7,12}; u_{10,12}$) based on their rankings are used to forecast the effective input at WT_{12}. Table 7 shows the performance metrics for short-term wind speed forecasting based on Jensen's, Frandsen's and proposed model.

For dataset D1, the RMSE for short-term wind forecasting without GRA is 5.86% with Jensen's model and 4.78% with Frandsen's model. With GRA, the RMSE for Jensen's model is 4.66% and for Frandsen's model it is 4.38%. The SSR/SST ratio was found better when wind forecasting in presence of wakes is done with GRA than without it. The performance metrics indicate that

Table 7: Forecasting results for wind turbine WT_{12} for dataset D1 and D2

Dataset	Metric	Jensen's model	
		without GRA	with GRA
D1	RMSE (%)	5.86	4.66
	SSR/SST	0.9866	1.0224
D2	RMSE (%)	8.06	6.86
	SSR/SST	1.0519	1.2934
		Frandsen's model	
		without GRA	with GRA
D1	RMSE (%)	4.78	4.38
	SSR/SST	1.0933	1.0818
D2	RMSE (%)	6.38	6.21
	SSR/SST	1.0297	1.3603
		Proposed model	
		without GRA	with GRA
D1	RMSE (%)	4.82	2.56
	SSR/SST	1.0599	1.0190
D2	RMSE (%)	5.52	4.72
	SSR/SST	1.0363	1.0150

wake modeling and wind forecasting based on Frandsen's model outperformed Jensen's model. Figures 14 and 15 show the forecasting results for wind turbine WT_{12} based on Jensen's, Frandsen's and Proposed model for datasets D1 and D2. Similarly for dataset D2, the RMSE without GRA for Jensen's model are 8.06%, while for Frandsen's model it was are 6.38%. With GRA, the RMSE for Jensen's model is 6.86% whereas for Frandsen's model it is 6.21%. It can be seen that RMSE for Frandsen's model is smaller than Jensen's model thus implying a better forecast in presence of wind wakes for turbine WT_{12}. The SSR/SST ratio is consistent for Jensen's and Frandsen's model and shows good agreement between actual and estimated values.

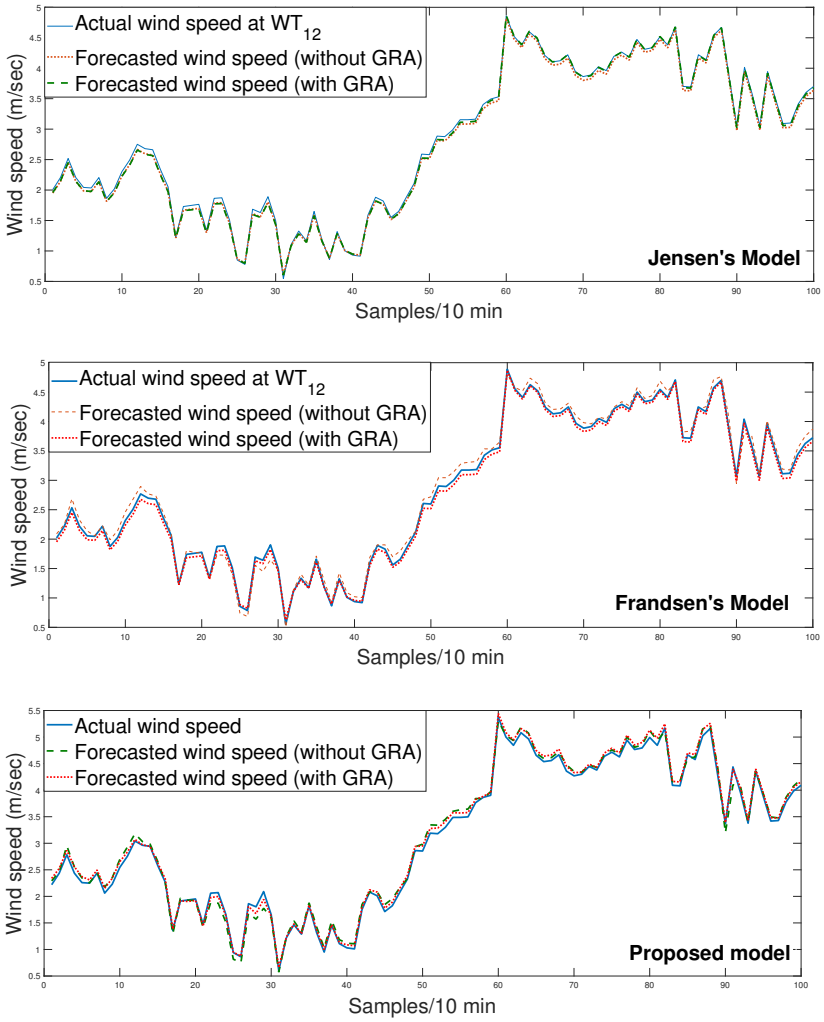

Figure 14: Wind forecasting for WT_{12} with and without GRA for dataset D1.

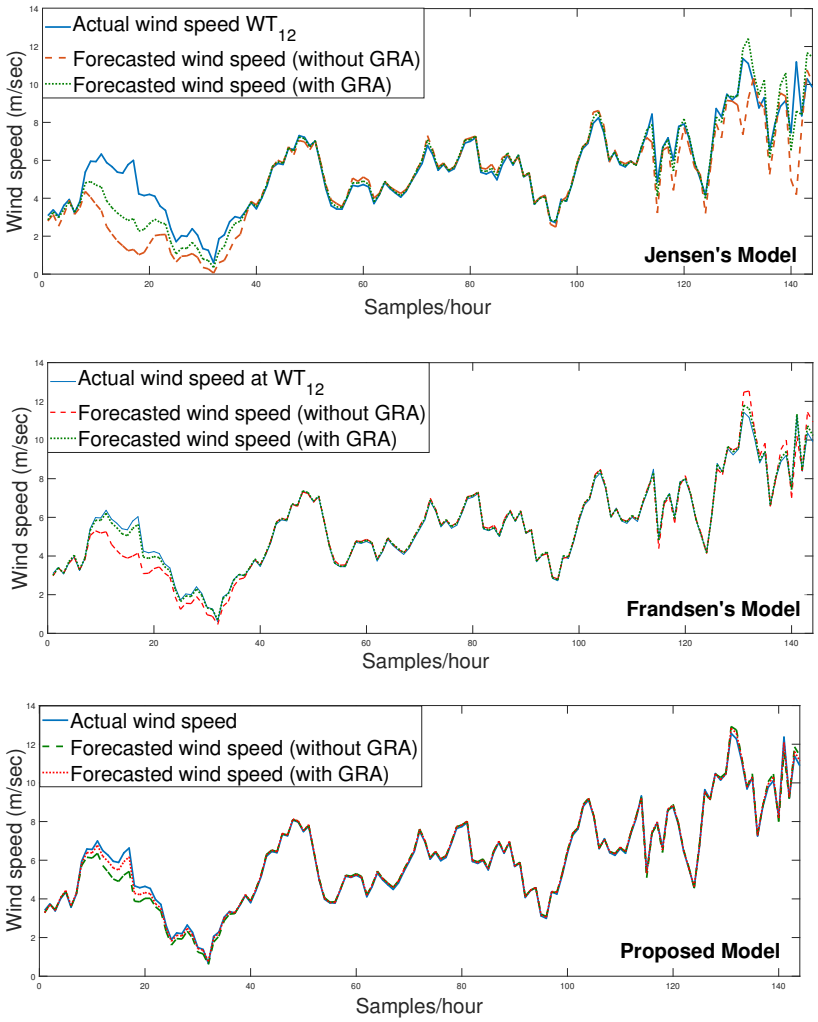

Figure 15: Wind forecasting for WT_{12} with and without GRA for dataset D2.

Based on our proposed model, we find that GRA analysis provides significantly better forecasting performance in terms of RMSE. The RMSE for dataset D1 is 4.82% without GRA and 2.56% with GRA. Similarly for dataset 2, the RMSE is 5.52% without GRA and 4.72% with GRA. For a 15-turbine wind farm layout the wind forecasting carried out for WT_{12} and we found that our proposed model yields better forecasting performance in presence of wind wakes.

5. Discussion

This paper discusses the short-term wind forecasting in presence of wakes by considering two different wind farm layouts and number of wind turbines. The wake effect is studied based on models proposed by Jensen and Frandsen. For single wake scenario, proposed bilateral Gaussian wake model is compared with Frandsen's and Jensen's model for different downwind distances. In a wind farm a downwind turbine experiences wakes due to multiple turbine thus creating a shadowing effect. Multiple wake scenario is tested for a 5-turbine wind farm layout and our proposed model outperformed Frandsen's model by 75.75% and Jensen's model by 91.75% in terms of RMSE. The short-term wind forecasting is carried out using a hybrid method based on wavelet decomposition and SVR. The inputs for the forecasting model are selected based on grey correlation degree and only significant inputs, that is, upwind turbines are selected as inputs to forecast wind speed for the downwind turbine. Based on our study we find that for both the wind farm layouts, with GRA, our proposed model outperforms Frandsen's and Jensen's model in terms of RMSE and choosing only significant upwind turbines as input to the SVR forecasting model we get much better forecast accuracy. The significance of grey correlation analysis in identifying wind turbines that actually cause velocity deficit, will lead to an efficient micro-siting of wind farms.

Limitations

Wind forecasting carried out in presence of wake interactions is studied. GRA is used to select input features for Support vector Regression based prediction model. SVR based forecasting however results in overestimating the wind speed predictions as indicated by SSR/SST index greater than 1. The over-fitting scenario of SVR can be possibly overcome by using improved variants of SVR like Least square support vector regression (LSSVR) and Twin support vector regression (TSVR).

6. Conclusion

A GRA based framework is use to study wind forecasting in presence of wind wakes. Benchmark wake models like Jensen's, Frandsen's models are tested against a novel Bilateral Gaussian wake model. The proposed wake model is based on Gaussian variation of Jensen's and Frandsen's models. The model is tested for two datasets D1 and D2 considering single wake and multiple wake scenario. The proposed model outperforms Jensen's and Frandsen's model. Further, forecasting is carried out where the wind speed time-series is decomposed into approximate and detail signals using daubechies wavelet with a 5-level decomposition. Wavelet transform removes the noise components present in the series and SVR is used to forecast wind speed. GRA is used as an important tool to identify the upstream turbines significantly contributing to wake effect. Results reveal that, for both the wind farm layouts, GRA improves the forecast accuracy.

References

[1] Chowdhury S, Zhang J, Messac A, Castillo L. Unrestricted wind farm layout optimization (UWFLO): Investigating key factors influencing the maximum power generation. Renewable Energy 2012;38(1):16–30.

[2] Manwell JF. Wind energy explained : theory, design and application. Chichester, U.K: Wiley; 2009. ISBN 978-0-470-01500-1.

[3] Archer CL, Vasel-Be-Hagh A, Yan C, Wu S, Pan Y, Brodie JF, et al. Review and evaluation of wake loss models for wind energy applications. Applied Energy 2018;226:1187–207.

[4] Hashemi-Tari P, Siddiqui K, Refan M, Hangan H. Wind tunnel investigation of the near-wake flow dynamics of a horizontal axis wind turbine. Journal of Physics: Conference Series 2014;524:012176.

[5] Ainslie J. Calculating the flowfield in the wake of wind turbines. Journal of Wind Engineering and Industrial Aerodynamics 1988;27(1-3):213–24.

[6] Larsen GC, Madsen HA, Thomsen K, Larsen TJ. Wake meandering: a pragmatic approach. Wind Energy 2008;11(4):377–95.

[7] Frandsen S, Barthelmie R, Pryor S, Rathmann O, Larsen S, Højstrup J, et al. Analytical modelling of wind speed deficit in large offshore wind farms. Wind Energy 2006;9(1-2):39–53.

[8] Sun H, Yang H. Study on an innovative three-dimensional wind turbine wake model. Applied Energy 2018;226:483–93.

[9] Barthelmie RJ, Larsen GC, Frandsen ST, Folkerts L, Rados K, Pryor SC, et al. Comparison of wake model simulations with offshore wind turbine wake profiles measured by sodar. Journal of Atmospheric and Oceanic Technology 2006;23(7):888–901.

[10] Tian L, Zhu W, Shen W, Zhao N, Shen Z. Development and validation of a new two-dimensional wake model for wind turbine wakes. Journal of Wind Engineering and Industrial Aerodynamics 2015;137:90–9.

[11] Ishihara T, Qian GW. A new gaussian-based analytical wake model for wind turbines considering ambient turbulence intensities and thrust coefficient effects. Journal of Wind Engineering and Industrial Aerodynamics 2018;177:275–92.

[12] Stevens RJ, Martínez-Tossas LA, Meneveau C. Comparison of wind farm large eddy simulations using actuator disk and actuator line models with wind tunnel experiments. Renewable Energy 2018;116:470–8.

[13] Porté-Agel F, Wu YT, Lu H, Conzemius RJ. Large-eddy simulation of atmospheric boundary layer flow through wind turbines and wind farms. Journal of Wind Engineering and Industrial Aerodynamics 2011;99(4):154–68.

[14] Wu YT, Porté-Agel F. Modeling turbine wakes and power losses within a wind farm using LES: An application to the horns rev offshore wind farm. Renewable Energy 2015;75:945–55.

[15] Rethore P, Sørensen N, Bechmann A, Zahle F. Study of the atmospheric wake turbulence of a cfd actuator disc model. In: EWEC 2009 Proceedings online. EWEC; 2009,.

[16] Stergiannis N, Lacor C, Beeck JV, Donnelly R. CFD modelling approaches against single wind turbine wake measurements using RANS. Journal of Physics: Conference Series 2016;753:032062.

[17] Göçmen T, van der Laan P, Réthoré PE, Diaz AP, Larsen GC, Ott S. Wind turbine wake models developed at the technical university of denmark: A review. Renewable and Sustainable Energy Reviews 2016;60:752–69.

[18] Schümann H, Pierella F, Sætran L. Experimental investigation of wind turbine wakes in the wind tunnel. Energy Procedia 2013;35:285–96.

[19] Crespo A, Hernndez J, Frandsen S. Survey of modelling methods for wind turbine wakes and wind farms. Wind Energy 1999;2(1):1–24.

[20] Barthelmie RJ, Hansen K, Frandsen ST, Rathmann O, Schepers JG, Schlez W, et al. Modelling and measuring flow and wind turbine wakes in large wind farms offshore. Wind Energy 2009;12(5):431–44.

[21] Porté-Agel F, Wu YT, Chen CH. A numerical study of the effects of wind direction on turbine wakes and power losses in a large wind farm. Energies 2013;6(10):5297–313.

[22] Park J, Law KH. Layout optimization for maximizing wind farm power production using sequential convex programming. Applied Energy 2015;151:320–34.

[23] Guan-yang L, Hongzhao W, Guanglei L, Yamei C, Hong-zheng L, Yi S. Security and stability analysis of wind farms integration into distribution network. IOP Conference Series: Materials Science and Engineering 2017;199:012102.

[24] Soman SS, Zareipour H, Malik O, Mandal P. A review of wind power and wind speed forecasting methods with different time horizons. In: North American Power Symposium 2010. IEEE; 2010,.

[25] Okumus I, Dinler A. Current status of wind energy forecasting and a hybrid method for hourly predictions. Energy Conversion and Management 2016;123:362–71.

[26] Zhou J, Shi J, Li G. Fine tuning support vector machines for short-term wind speed forecasting. Energy Conversion and Management 2011;52(4):1990–8.

[27] Du P, Wang J, Yang W, Niu T. A novel hybrid model for short-term wind power forecasting. Applied Soft Computing 2019;80:93–106. URL: https://doi.org/10.1016/j.asoc.2019.03.035. doi:10.1016/j.asoc.2019.03.035.

[28] Wang J, Zhang W, Li Y, Wang J, Dang Z. Forecasting wind speed using empirical mode decomposition and elman neural network. Applied Soft Computing 2014;23:452–9.

[29] Liu H, Chen C, qi Tian H, fei Li Y. A hybrid model for wind speed prediction using empirical mode decomposition and artificial neural networks. Renewable Energy 2012;48:545–56.

[30] Wang S, Zhang N, Wu L, Wang Y. Wind speed forecasting based on the hybrid ensemble empirical mode decomposition and GA-BP neural network method. Renewable Energy 2016;94:629–36.

[31] Wang J, Du P, Niu T, Yang W. A novel hybrid system based on a new proposed algorithm—multi-objective whale optimization algorithm for wind speed forecasting. Applied Energy 2017;208:344–60.

[32] Jensen N. A note on wind generator interaction. 1983. ISBN 87-550-0971-9.

[33] Stull RB, editor. An Introduction to Boundary Layer Meteorology. Springer Netherlands; 1988.

[34] Wu YT, Porté-Agel F. Atmospheric turbulence effects on wind-turbine wakes: An LES study. Energies 2012;5(12):5340–62.

[35] Bastankhah M, Porté-Agel F. A new analytical model for wind-turbine wakes. Renewable Energy 2014;70:116–23.

[36] Sizhuang L, Youtong F. Analysis of the jensen's model, the frandsen's model and their gaussian variations. In: 2014 17th International Conference on Electrical Machines and Systems (ICEMS). IEEE; 2014,.

[37] Sathe A, Mann J, Barlas T, Bierbooms W, van Bussel G. Influence of atmospheric stability on wind turbine loads. Wind Energy 2012;16(7):1013–32.

[38] González-Longatt F, Wall P, Terzija V. Wake effect in wind farm performance: Steady-state and dynamic behavior. Renewable Energy 2012;39(1):329–38.

[39] Markfort CD, Zhang W, Porté-Agel F. Turbulent flow and scalar transport through and over aligned and staggered wind farms. Journal of Turbulence 2012;13:N33.

[40] He Q, Wang J, Lu H. A hybrid system for short-term wind speed forecasting. Applied Energy 2018;226:756–71.

[41] Yin SF, jing Wang X, hui Wu J, li Wang G. Grey correlation analysis on the influential factors the hospital medical expenditure. In: Information Computing and Applications. Springer Berlin Heidelberg; 2010, p. 73–8.

[42] Mohandes M, Halawani T, Rehman S, Hussain AA. Support vector machines for wind speed prediction. Renewable Energy 2004;29(6):939–47.

[43] Mi XW, Liu H, fei Li Y. Wind speed forecasting method using wavelet, extreme learning machine and outlier correction algorithm. Energy Conversion and Management 2017;151:709–22.

[44] Li H, Wang J, Lu H, Guo Z. Research and application of a combined model based on variable weight for short term wind speed forecasting. Renewable Energy 2018;116:669–84.

[45] Liu JP, xiao Niu D, yun Zhang H, qing Wang G. Forecasting of wind velocity: An improved SVM algorithm combined with simulated annealing. Journal of Central South University 2013;20(2):451–6.

[46] Wavelet transform. In: Signal Analysis. John Wiley & Sons, Ltd; ????, p. 210–64.

[47] Vapnik VN. The Nature of Statistical Learning Theory. Springer New York; 2000.

[48] Duan H, Wang R, Liu X, Liu H. A method to determine the hyperparameter range for tuning RBF support vector machines. In: 2010 International Conference on E-Product E-Service and E-Entertainment. IEEE; 2010,.